

International Journal of Modern Physics A
© World Scientific Publishing Company

Charm Dalitz analyzes from CLEO-c *

Mikhail Dubrovin

Wayne State University, 666 W. Hancock St
Detroit, 48201 MI, U.S.A.
dubrovin@mail.lepp.cornell.edu

CLEO Collaboration

Wilson Synchrotron Laboratory, Cornell University
Ithaca, NY 14853, U.S.A.

August 18, 2019

I discuss CLEO-c opportunities in Dalitz plot analyzes with the data samples available now and projected by the end of CESR-c run. Using 281 pb^{-1} of e^+e^- collisions at mass of $\psi(3770)$ we present results of the Dalitz plot analysis of $D^+ \rightarrow \pi^- \pi^+ \pi^+$. Using the CLEO-c and CLEO III samples of 5 pb^{-1} , accrued at mass of $\psi(2S)$, we study three body decays of χ_{cJ} produced in the radiative decay $\psi(2S) \rightarrow \gamma \chi_{cJ}$, where $J=0,1,2$. A clear signal from at least one of χ_{cJ} is found in eight final states: $\pi^+ \pi^- \eta$, $\pi^+ \pi^- \eta'$, $K^+ K^- \pi^0$, $K_S^0 K \pi$, $\eta K^+ K^-$, $\pi^0 p \bar{p}$, $\eta p \bar{p}$, and $\Lambda K^+ \bar{p}$. For these modes we measured or set an upper limit on the branching fraction. A Dalitz plot analysis is performed on three modes $\chi_{c1} \rightarrow \pi^+ \pi^- \eta$, $K^+ K^- \pi^0$, and $K_S^0 K \pi$.

Keywords: charmonium; meson; production; decay; Dalitz; CLEO; experiment.

PACS numbers: 13.25.Ft, 13.25.Gv, 13.25.Jx, 13.60.Le, 13.66.Bc

1. The CLEO-c opportunities in Dalitz plot analyzes

Currently the CLEO collaboration possesses multiple samples of data which can be used for analysis of D , D_s , χ_{cJ} , J/ψ meson decays.

- A sample of $e^+e^- \rightarrow \psi(3770) \rightarrow D\bar{D}$ events with integrated luminosity of 281 pb^{-1} , which is equivalent to $\sim 10^6$ of D^+D^- , and $0.8 \cdot 10^6$ of $D^0\bar{D}^0$ pairs. We find about 20 three-body decay modes of charged and neutral D mesons to the combinations of π , K , and η in the final state that can be used for the Dalitz plot analysis. Running at $D\bar{D}$ production threshold gives many advantages. There is no extra-energy for production of additional fragmentation particles which keeps the multiplicity low and gives very clean events. In some cases, where combinatoric background is small, we use inclusive reconstruction of a single D meson. In exclusive modes one D meson of $D\bar{D}$ pair can be used as a flavor or CP tag¹, and the

*Presented at Charm-2006 conference, June 5-7, IHEP, Beijing, China.

recoiling D studied.

- A sample of $e^+e^- \rightarrow D_s^* \overline{D}_s$ events at $\sqrt{s} = 4170$ MeV with $\mathcal{L} \simeq 200 \text{ pb}^{-1}$, or $2 \cdot 10^5$ of $D_s^* \overline{D}_s$ (charge conjugated modes are implied throughout this paper). This sample has been collected during Spring of this year and its processing is still in progress. We are going to use D_s mesons for the Dalitz plot analysis. In particular, for the decay mode $D_s^+ \rightarrow \phi \pi^+$, often used as a reference, an interference with other modes can be studied in the amplitude analysis of the $D_s^+ \rightarrow K^+ K^- \pi^+$ decay.
- A sample of $e^+e^- \rightarrow \psi(2S)$ events with $\mathcal{L} \simeq 5 \text{ pb}^{-1}$, or 3 million produced $\psi(2S)$'s which can be used to study J/ψ or χ_{cJ} decays in the processes

- ▷ $\psi(2S) \rightarrow \pi\pi J/\psi$ with $\mathcal{B} \simeq 50\%$ for $\pi^+\pi^-$ and $\pi^0\pi^0$ together,
- ▷ $\psi(2S) \rightarrow \gamma\chi_{cJ}$ with $\mathcal{B} \simeq 9\%$ for each spin $J = 0, 1, 2$ state.

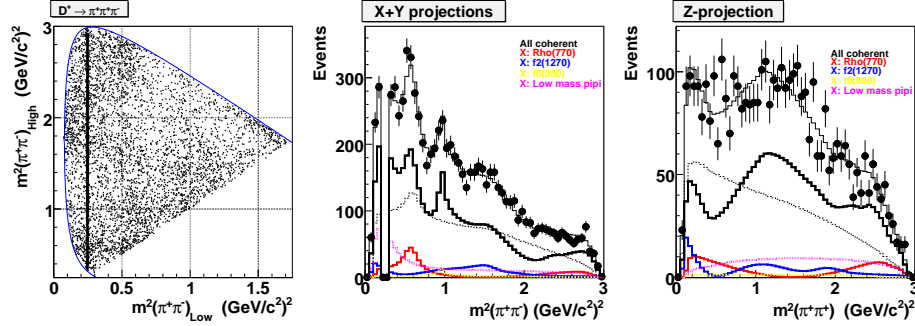
The $\pi\pi$ pair in the first case and the γ in the second can be used as an additional signal tag for these processes. A partial wave analysis can be applied in order to study decay of particle with non-zero spin, but as a first step, with this small sample in hand, we perform Dalitz plot analyzes with a special treatment of angular distributions.

The current CLEO-c run plan has running on the $\psi(2S)$ completed during the fall of 2006 accumulating ten times more statistics of $\psi(2S)$. By the end of the CLEO-c program (April 2008) we are going to gather samples of $D\overline{D}$ three and $D_s^* \overline{D}_s$ four times larger than we have at present. This data size and cleanliness is encouraging us to proceed with decay substructure study in 3-body decay modes using the Dalitz plot technique². At this conference we present preliminary results of a few Dalitz plot analyzes of the decays $D^+ \rightarrow \pi^- \pi^+ \pi^+$ and $\chi_{c1} \rightarrow \pi^+ \pi^- \eta$, $K^+ K^- \pi^0$, and $K_S^0 K \pi$.

2. Dalitz plot analysis of $D^+ \rightarrow \pi^- \pi^+ \pi^+$

A Dalitz plot analysis of $D^+ \rightarrow \pi^- \pi^+ \pi^+$ has previously been done by E791³ and FOCUS⁴. The preliminary analysis described here is from CLEO-c⁵, and represents the first time we have done the same Dalitz plot analysis as the fixed target experiments. The decay is selected with cuts on the beam constrained mass of three charged tracks consistent with pions, $m_{BC} = \sqrt{E_{beam}^2 - p^2(\pi^- \pi^+ \pi^+)}$, and the difference of their energy from the beam energy, $\Delta E = E(\pi^- \pi^+ \pi^+) - E_{beam}$. A sample of 6991 events is selected with a signal to noise of about two to one. The E791 and FOCUS samples are of similar size and cleanliness.

The Dalitz plot is symmetric under the interchange of like-sign pions thus we do the fit in the two dimensions of high versus low unlike-sign pion mass, as shown in Fig. 1(left). There is a large contribution from $D^+ \rightarrow K_S^0 \pi^+$ which because of the long K_S^0 lifetime should not interfere with other submodes. We do not consider events with $m(\pi^+ \pi^-)$ within ten standard deviations in mass resolution of the known K_S^0 mass on the Dalitz plot. This leaves 4068 events which are shown in the projection plots of Fig. 1. An unbinned maximum likelihood fit is used along with

Fig. 1. Dalitz plot and projections for $D^+ \rightarrow \pi^- \pi^+ \pi^+$.

other methods as described in Ref. ⁶. The efficiency across the Dalitz plot is modeled with simulated events that are fit to a two-dimensional second order polynomial and threshold functions to account the fall off at the corners. Backgrounds are taken from m_{BC} and ΔE sidebands and extra resonance contributions are allowed from mis-measured K_S^0 , ρ , and $f_2(1270)$ decays. A total of 13 different resonances are considered. Parameters describing these resonances are taken from previous experiments. Only contributions with an amplitude significant at more than three standard deviations are said to be observed, and others are limited. Contributions that are not significant are not included in the decay model used for the result.

Contributions from $\rho^0\pi$, $f_0(980)\pi$, and $f_2(1270)\pi$ are clearly visible. Table 1 shows the preliminary amplitudes, phases, and fit fractions measured by CLEO compared with the results of the E791 analysis mentioned above. There is broad

Table 1. Summary of results for $D^+ \rightarrow \pi^- \pi^+ \pi^+$.

Mode	Amplitude	Phase ($^\circ$)	Fit Fraction (%)	E791: Fit Fraction (%)
$\rho(770)\pi^+$	1(fixed)	0(fixed)	$20.0 \pm 2.3 \pm 0.9$	33.6 ± 3.9
$f_0(980)\pi^+$	$1.4 \pm 0.2 \pm 0.2$	$12 \pm 10 \pm 5$	$4.1 \pm 0.9 \pm 0.3$	6.2 ± 1.4
$f_2(1270)\pi^+$	$2.1 \pm 0.2 \pm 0.1$	$-123 \pm 6 \pm 3$	$18.2 \pm 2.6 \pm 0.7$	19.4 ± 2.5
$f_0(1370)\pi^+$	$1.3 \pm 0.4 \pm 0.2$	$-21 \pm 15 \pm 14$	$2.6 \pm 1.8 \pm 0.6$	2.3 ± 1.7
$f_0(1500)\pi^+$	$1.1 \pm 0.3 \pm 0.2$	$-44 \pm 13 \pm 16$	$3.4 \pm 1.0 \pm 0.8$	—
$\sigma\pi^+$	$3.7 \pm 0.3 \pm 0.2$	$-3 \pm 4 \pm 2$	$41.8 \pm 1.4 \pm 2.5$	46.3 ± 9.2
Non-resonant			< 3.5	7.8 ± 6.6
$\rho(1450)\pi^+$			< 2.4	0.7 ± 0.8
$\sum_i FF_i, \%$			90.2	116

agreement between the two results, including the observation of a $\sigma\pi$ contribution. In an alternative fit using the same decay model as E791 the agreement is only slightly better, but the fit is much less likely to model our data than the model shown in the table which does not include non-resonant and $\rho(1450)\pi^+$ contributions, but does include a $f_0(1500)\pi^+$ contribution. Models without a $\sigma\pi$ contribution do not agree well with the data.

This CLEO analysis is preliminary, and we plan to consider a generalized model

of $\pi^+\pi^-$ S-wave interactions to model σ and f_0 contributions such as the K-matrix which is used in the FOCUS analysis mentioned above.

3. Three-body decays of χ_{cJ}

Decays of the χ_{cJ} states are not well studied both experimentally and theoretically. Assuming that χ_{cJ} are the 3P_J $c\bar{c}$ -bound states one would expect that χ_{c0} and χ_{c2} with J^{PC} quantum numbers 0^{++} and 2^{++} decay to the light quarks via two gluons⁷. Measurement of any possible χ_{cJ} hadronic decays provides valuable information on possible glueball dynamics.

We study the decay modes of χ_{cJ} using the process $e^+e^- \rightarrow \psi(2S) \rightarrow \gamma\chi_{cJ}$ with 3 million $\psi(2S)$ produced. We search for signals in the $\chi_{cJ} \rightarrow h^0 h^+ h^-$ three-body decays, where h^0 stands for π^0 , K_s^0 , η , η' or Λ , and h^+ is π^+ , K^+ or p .

Our basic technique is an exclusive analysis. A photon candidate is combined with three hadrons and the 4-momentum sum constrained to the known beam energy and small momentum caused by the beam crossing angle. We cut on the χ^2 of this fit, which has four degrees of freedom, as it strongly discriminates between background and signal. Efficiencies and backgrounds are studied in a GEANT-based simulation of the detector's full response. Our simulated sample is roughly ten times our data sample. The simulation is generated with a $1 + \lambda \cos^2 \theta$ distribution in $\cos \theta$, where θ is the radiated photon angle relative to the positron beam axis. A E1 transition, as expected for $\psi(2S) \rightarrow \gamma\chi_{cJ}$, implies $\lambda = 1, -1/3, +1/13$ for $J = 0, 1, 2$ particles. The differences of efficiencies due to various θ distributions are negligible as we accept transition photons down to our detection limit.

We use standard CLEO algorithms for tracks reconstruction in the tracking system and photons in CsI calorimeter. Combined dE/dx and RICH, E/p are exploited for particle identification and background suppression. π^0 's are formed from two photon candidates of the $\pi^0 \rightarrow \gamma\gamma$ decay. We use $\eta \rightarrow \gamma\gamma$ and $\eta \rightarrow \pi^+\pi^-\pi^0$ decays to reconstruct η mesons. The η' candidates are formed from $\eta' \rightarrow \eta\pi^+\pi^-$ and $\eta' \rightarrow \gamma\rho$ (with $E_\gamma > 200$ MeV, and $\pi^+\pi^-$ mass to be within 100 MeV/ c^2 of the ρ mass) combinations. In most cases mass constrained fits are applied with appropriate cut on χ^2 value. $K_S^0 \rightarrow \pi^+\pi^-$ and $\Lambda \rightarrow p\pi^-$ candidates are formed from good quality tracks that are constrained to come from a common vertex. The K_S^0 flight path is required to be greater than 5 mm and the Λ flight path greater than 3 mm. The mass cut around the K_S^0 mass is ± 10 MeV/ c^2 , and around the Λ mass ± 5 MeV/ c^2 . Events with only the correct number of selected tracks for the decay mode being considered are accepted.

The efficiencies averaged over the CLEO III and CLEO-c data sets for each mode, including the branching fractions of $\eta \rightarrow \gamma\gamma$, $\eta \rightarrow \pi^+\pi^-\pi^0$ and $\eta' \rightarrow \eta\pi^+\pi^-$, are in the range 8% to 30%.

Figure 2 shows the mass distributions with fits for the eight χ_{cJ} decay modes. Signals are evident in all three χ_{cJ} states, but not in all the modes. Backgrounds are small. The mass distributions are fit to three signal shapes, Breit-Wigners convolved

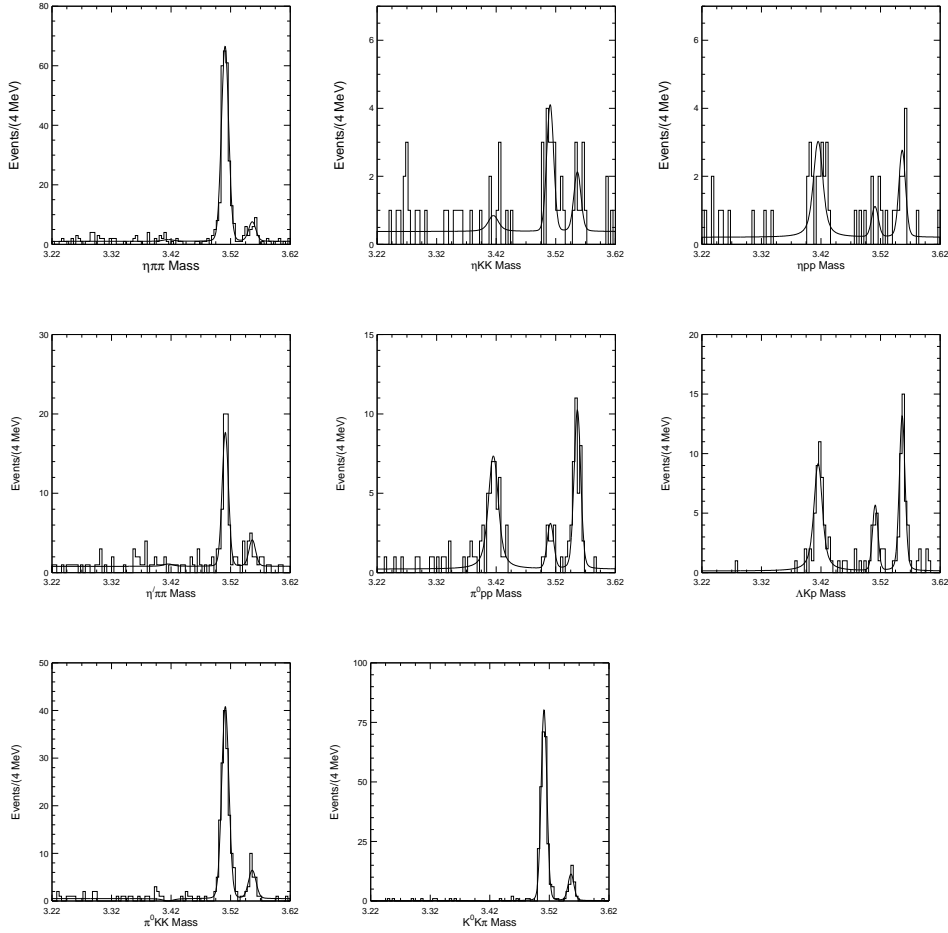


Fig. 2. Mass distribution for candidate $\chi_{cJ} \rightarrow \pi^+\pi^-\eta$, $K^+K^-\eta$, $p\bar{p}\eta$, $\pi^+\pi^-\eta'$, $p\bar{p}\pi^0$, $K^+\bar{p}\Lambda$, $K^+K^-\pi^0$, and $K_S^0K^-\pi^+$.

with Gaussian detector resolutions (with σ from 4.3 to 7 MeV/ c^2 , depending on mode), and a linear background. The χ_{cJ} masses and intrinsic widths are fixed at the values from Ref. ⁸.

We consider various sources of systematic uncertainties on the yields: allowing the χ_{cJ} masses and intrinsic widths to float in the fit; change the shape of background; break up the sample into CLEO III and CLEO-c data sets; uncertainty on the efficiency of photon and track reconstruction; uncertainty due to the cut on the χ^2 in mass and event vertex constrained fits. Based on the results of the Dalitz plot analyzes we correct the efficiency in the $\chi_{c1} \rightarrow \pi^+\pi^-\eta$, $\chi_{c1} \rightarrow K^+K^-\pi^0$, and $\chi_{c1} \rightarrow K_S^0K^-\pi^+$ modes by a relative up to 6% to account for the change in the

efficiency caused by the deviation from a uniform phase space distribution of decay products to what we actually observe. To calculate χ_{cJ} branching fractions, we use previous CLEO measurements⁹ for the $\psi(2S) \rightarrow \gamma\chi_{cJ}$ branching fractions of $9.33 \pm .14 \pm .61\%$, $9.07 \pm .11 \pm .54\%$ and $9.22 \pm .11 \pm .46\%$ for $J = 0, 1, 2$ respectively. Preliminary results for the three body branching fractions are shown in Table 2. Where the yields do not show clear signals we calculate 90% confidence level upper limits accounting for statistical and systematic uncertainties.

Table 2. Preliminary branching fractions in %. Uncertainties are statistical, systematic, and a separate systematic due to uncertainties in the $\psi(2S)$ branching fractions. Limits are at the 90% confidence level.

Mode	χ_{c0}	χ_{c1}	χ_{c2}
$\pi^+\pi^-\eta$	< 0.021	$0.52 \pm .03 \pm .03 \pm .03$	$0.051 \pm .011 \pm .004 \pm .003$
$K^+K^-\eta$	< 0.024	$0.034 \pm .010 \pm .003 \pm .002$	< 0.033
$p\bar{p}\eta$	$0.038 \pm .010 \pm .003 \pm .02$	< 0.015	$.019 \pm .007 \pm .002 \pm .002$
$\pi^+\pi^-\eta'$	< 0.038	$0.24 \pm .03 \pm .02 \pm .02$	< 0.053
$K^+K^-\pi^0$	< 0.006	$0.200 \pm .015 \pm .018 \pm .014$	$0.032 \pm .007 \pm .002 \pm .002$
$\bar{K}^0K^-\pi^+$	< 0.010	$0.84 \pm .05 \pm .06 \pm .05$	$0.15 \pm .02 \pm .01 \pm .01$
$p\bar{p}\pi^0$	$0.059 \pm .010 \pm .006 \pm .004$	$0.014 \pm .005 \pm .001 \pm .001$	$0.045 \pm .007 \pm .004 \pm .003$
$K^+\bar{p}\Lambda$	$0.114 \pm .016 \pm .009 \pm .007$	$0.034 \pm .009 \pm .003 \pm .002$	$0.088 \pm .014 \pm .07 \pm .006$

4. Dalitz plot analysis of $\chi_{c1} \rightarrow \pi^+\pi^-\eta$, $K^+K^-\pi^0$, and $K_S^0K\pi$

We choose the three high statistics signals $\chi_{c1} \rightarrow \pi^+\pi^-\eta$, $\chi_{c1} \rightarrow K^+K^-\pi^0$, and $\chi_{c1} \rightarrow K_S^0K^-\pi^+$ with 228, 137, and 234 events respectively for Dalitz plot analyzes to study resonance substructure. Events were selected within 10 MeV, roughly two standard deviations, of the signal peak. When fitting the data Dalitz plot the small contributions from backgrounds are neglected. We use an isobar model to describe resonance contributions taking into account spin and width dependent effects. Narrow resonances are described with a Breit-Wigner amplitude with the resonance parameters taken from previous experiments⁸. We use the Flatté line-shape for $a_0(980)$ with parameters from the Crystal Barrel Collaboration¹⁰. For low mass $\pi^+\pi^-(\sigma)$ and $K\pi(\kappa)$ S-wave contributions we choose a simple description which is adequate for our small sample¹¹.

We are examining the $e^+e^- \rightarrow \psi(2S) \rightarrow \gamma\chi_{c1}$ process. In such a decay the χ_{c1} should be polarized. For our small sample we use angular distributions from¹², calculated for non-polarized χ_{c1} decay. We have tested different angular distributions and include the variations as a systematic uncertainty.

Fig. 3 shows the Dalitz plot and three projections for $\chi_{c1} \rightarrow \pi^+\pi^-\eta$. There are clear contributions from $a_0(980)^\pm\pi^\mp$ and $f_2(1270)\eta$ intermediate states, and significant accumulation of events at low $\pi^+\pi^-$ mass. Isospin symmetry predicts that amplitudes and strong phases of both charge conjugated states should be equal. The overall amplitude normalization and one phase are arbitrary parameters and we set $a_{a_0(980)^+} = a_{a_0(980)^-} = 1$, $\phi_{a_0(980)^+} = \phi_{a_0(980)^-} = 0$. All other fit components

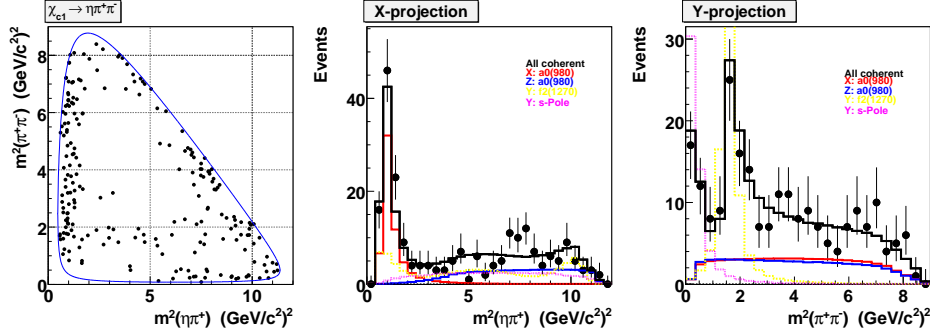


Fig. 3. Dalitz plot and projections on the two mass squared combinations for $\chi_{c1} \rightarrow \pi^+ \pi^- \eta$.

are defined with respect to this choice for $a_0(980)$.

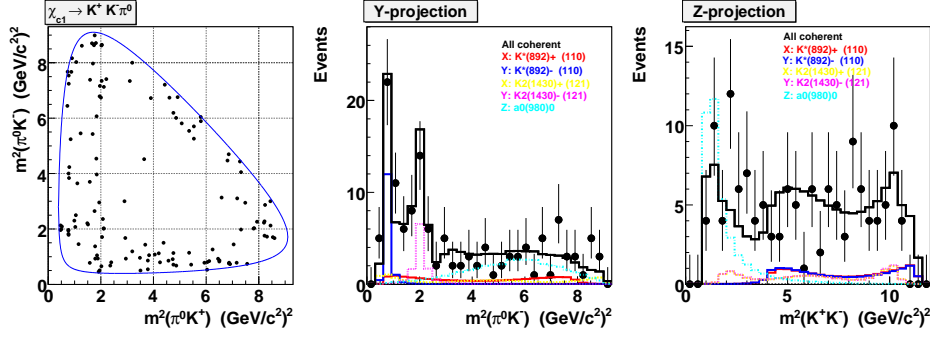
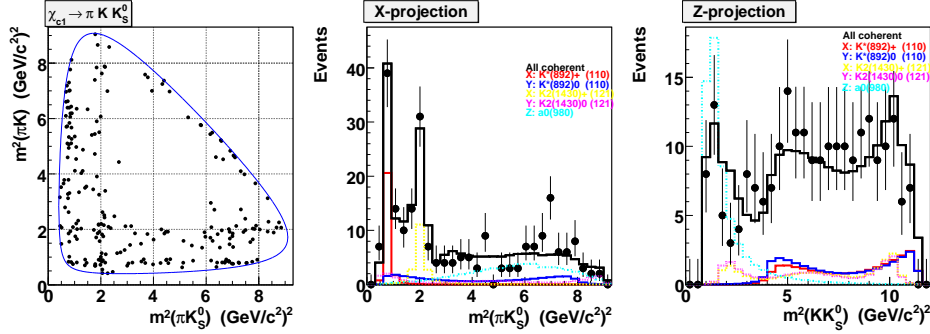
Our initial fit to this mode includes only $a_0(980)^\pm \pi^\mp$ and $f_2(1270)\eta$ contributions, but has a low probability of describing the data, 0.13%, due to the accumulation of events at low $\pi^+ \pi^-$ mass. We find that only the $\sigma\eta$ describes well the low $\pi^+ \pi^-$ mass spectrum, and finally describe the Dalitz plot with $a_0(980)^\pm \pi^\mp$, $f_2(1270)\eta$, and $\sigma\eta$ contributions. Table 3 gives the preliminary results of this fit which has a probability to match the data of 58%. Systematic uncertainties shown in Table 3 were estimated from variations to nominal fit results in numerous cross-checks. We consider variation of the efficiency shape, uncertainties in resonance parameters, presence of additional resonances etc. We note that with higher statistics this mode may offer one of the best measurements of the parameters of the $a_0(980)$.

Table 3. Preliminary fit results for $\chi_{c1} \rightarrow \pi^+ \pi^- \eta$ Dalitz plot analysis. The uncertainties are statistical and systematic.

Contribution	Amplitude	Phase ($^\circ$)	Fit Fraction (%)
$a_0(980)^\pm \pi^\mp$	1	0	$56.2 \pm 3.6 \pm 1.4$
$f_2(1270)\eta$	$0.186 \pm 0.017 \pm 0.003$	$-118 \pm 10 \pm 4$	$35.1 \pm 2.9 \pm 1.8$
$\sigma\eta$	$0.68 \pm 0.07 \pm 0.05$	$-85 \pm 18 \pm 15$	$21.7 \pm 3.3 \pm 0.5$

The Dalitz plot for $\chi_{c1} \rightarrow K^+ K^- \pi^0$ decay and its projections are shown in Fig. 4, and for $\chi_{c1} \rightarrow K_S^0 K^- \pi^+$ in Fig. 5. We do a combined Dalitz plot analysis to these modes taking into account isospin symmetry on amplitudes and phases: $a_{K^{*+}} = a_{K^{*-}} = a_{K^{*0}} = a_{\overline{K^{*0}}} \equiv a_{K^*}$, $\phi_{K^{*+}} = \phi_{K^{*-}} = \phi_{K^{*0}} = \phi_{\overline{K^{*0}}} \equiv \phi_{K^*}$, $a_{a(980)^+} = a_{a(980)^-} = a_{a(980)^0} \equiv a_{a(980)}$, and $\phi_{a(980)^+} = \phi_{a(980)^-} = \phi_{a(980)^0} \equiv \phi_{a(980)}$. The common relative factor between two Dalitz plot amplitudes does not matter because of each Dalitz plot has an arbitrary normalization. The overall amplitude normalization and one phase are arbitrary parameters and we set $a_{K^*(892)} = 1$ and $\phi_{K^*(892)} = 0$.

The limited size of this sample, even in the combined Dalitz plot analysis, and the many possible contributing resonances leave us unable to draw clear conclu-

Fig. 4. Dalitz plot and projections on the two mass squared combinations for $\chi_{c1} \rightarrow K^+ K^- \pi^0$.Fig. 5. Dalitz plot and projections on the two mass squared combinations for $\chi_{c1} \rightarrow K_S^0 K^- \pi^+$.

sions. Visual inspection shows clear contributions from $K^*(892)^\pm K^\mp$, $K^*(892)^0 K_S^0$, $K^*(1430)^\pm K^\mp$, $K^*(1430)^0 K_S^0$, $a_0(980)^0 \pi^0$, and $a_0(980)^\pm \pi^\mp$. It is not clear that the $K^*(1430)$ are K_0^* or K_2^* , and many other $K\pi$ and KK resonances can possibly contribute. Our best fit preliminary result is presented in Table 4 showing statis-

Table 4. Preliminary results of the combined fits to the $\chi_{c1} \rightarrow K^+ K^- \pi^0$ and $\chi_{c1} \rightarrow K_S^0 K^- \pi^+$ Dalitz plots.

Contribution	Amplitude	Phase ($^\circ$)	Fit Fraction (%)
$K^*(892)K$	1	0	$19.7 \pm 4.0 \pm 2.0$
$K_2^*(1430)K$	$0.50 \pm 0.09 \pm 0.12$	$-2 \pm 13 \pm 6$	$18.0 \pm 6.6 \pm 3.2$
$K_0^*(1430)K$	$5.3 \pm 1.0 \pm 0.1$	$77 \pm 12 \pm 16$	$36.0 \pm 12.8 \pm 3.0$
$K^*(1680)K$	$2.3 \pm 0.5 \pm 0.5$	$-38 \pm 12 \pm 12$	$11.2 \pm 5.4 \pm 2.7$
$a_0(980)\pi$	$10.8 \pm 1.2 \pm 1.2$	$-112 \pm 12 \pm 3$	$29.5 \pm 7.1 \pm 2.6$

tical and systematic errors. This fit has a good 32% probability of matching the data and agrees with fits done to the separate Dalitz plots not taking advantage of isospin symmetry. We also find that an alternative solution using the same set of contributions fits the data acceptably, but less well than the displayed result.

5. Summary

The CLEO collaboration possesses data samples which can be used for analysis of D , D_s , χ_{cJ} , J/ψ meson decays. Using roughly 10^6 of D^+D^- pairs produced in the $e^+e^- \rightarrow \psi(3770) \rightarrow D\bar{D}$ process we perform a Dalitz plot analysis of the $D^+ \rightarrow \pi^-\pi^+\pi^+$ decay. We confirm a dominant contribution from a low mass $\pi^+\pi^-$ S-wave amplitude earlier observed by E791 and FOCUS experiments. Results of the $D^+ \rightarrow \pi^-\pi^+\pi^+$ Dalitz plot analysis are summarized in Table 1.

We have searched for and studied selected three body hadronic decays of the χ_{c0} , χ_{c1} , χ_{c2} produced in radiative decays of the $\psi(2S)$ in e^+e^- collisions observed with the CLEO detector. The clean signal at least for one of χ_{cJ} 's is found in eight final states: $\pi^+\pi^-\eta$, $\pi^+\pi^-\eta'$, $K^+K^-\pi^0$, $K_S^0K\pi$, ηK^+K^- , $\pi^0 p\bar{p}$, $\eta p\bar{p}$, and $\Lambda K^+\bar{p}$. Our preliminary observations and branching fraction limits are summarized in Table 2. In $\chi_{c1} \rightarrow \pi^+\pi^-\eta$ we have studied the resonant substructure using a Dalitz plot analysis, and our preliminary results are summarized in Table 3. Similarly in $\chi_{c1} \rightarrow KK\pi$ we clearly see contributions from $K^*(892)K$ and $a_0(980)\pi$ at roughly the 20% and 30% level respectively, as shown in Table 4.

Acknowledgments

We gratefully acknowledge the effort of the CESR staff in providing us with excellent luminosity and running conditions. D. Cronin-Hennessy and A. Ryd thank the A.P. Sloan Foundation. This work was supported by the National Science Foundation, the U.S. Department of Energy, and the Natural Sciences and Engineering Research Council of Canada.

References

1. M. Gronau, Y. Grossman and J.L. Rosner, Phys.Lett. **B 508** (2001) 37.
2. R.H.Dalitz, Phil. Mag. **44** (1953) 1068.
3. E.M.Aitala *et al.* (Fermilab E791 Collaboration), Phys. Rev. Lett. **86** (2001) 770.
4. J.M.Link *et al.* (FOCUS Collaboration), Phys. Lett. **B 585** (2004) 200.
5. R.A. Briere *et al.* (CESR-c and CLEO-c Taskforces, CLEO-c Collaboration), Cornell University, LEPP Report No. CLNS 01/1742 (2001) (unpublished).
6. S. Kopp *et al.*, Phys. Rev. **D 63**, 092001 (2001).
7. N. Brambilla *et al.*, CERN-2005-005 [hep-ph/0412158] is a comprehensive recent review of heavy quarkonium physics.
8. S. Eidelman *et al.*, Physics Letters **B 592**, 1 (2004).
9. S.B. Athar *et al.*, (CLEO Collaboration), Phys. Rev. **D 70**, 112002 (2004).
10. Crystal Barrel Collaboration, Phys. Rev. **D 57** (1998) 3860.
11. J.A. Oller, Phys. Rev. **D 71**, 054030 (2005).
12. V. Filippini, A. Fontana, and A. Rotondi, Phys. Rev. **D 51** (1995) 2247.